


# PROCEEDINGS REPRINT

 SPIE—The International Society for Optical Engineering

*11/27/95*  
*11/27/95*  
*11/27/95*

*Reprinted from*

## ***EUV, X-Ray, and Gamma-Ray Instrumentation for Astronomy VI***

**12–14 July 1995  
San Diego, California**



**Volume 2518**



# The Extreme Ultraviolet Spectrograph Sounding Rocket Payload: Recent Modifications for Planetary Observations in the EUV/FUV

David C. Slater, S. Alan Stern, and John Scherrer

Instrumentation and Space Research Division  
Southwest Research Institute  
6220 Culebra Rd.  
P.O. Drawer 28510  
San Antonio, TX 78228-0510  
USA

and

Webster Cash, James C. Green, and Erik Wilkinson

Center for Astrophysics and Space Astronomy  
University of Colorado  
Boulder, CO 80309

## ABSTRACT

We report on the status of modifications to an existing extreme ultraviolet (EUV) telescope/spectrograph sounding rocket payload for planetary observations in the 800 – 1200 Å wavelength band. The instrument is composed of an existing Wolter Type II grazing incidence telescope, a newly built 0.4-m normal incidence Rowland Circle spectrograph, and an open-structure resistive-anode microchannel plate detector. The modified payload has successfully completed three NASA sounding rocket flights within 1994-1995. Future flights are anticipated for additional studies of planetary and cometary atmospheres and interstellar absorption. A detailed description of the payload, along with the performance characteristics of the integrated instrument are presented. In addition, some preliminary flight results from the above three missions are also presented.

**Keywords:** Extreme Ultraviolet, Far Ultraviolet, VUV spectroscopy, EUV instrumentation, sounding rocket, Jupiter/Io torus, Venus, Spica

## 1. INTRODUCTION

The region of the UV between 500 and 1200 Å is a rich one for the study of planetary and astrophysical targets. Extreme and far ultraviolet (EUV and FUV) atmospheric spectroscopy opens up an important window on ion and neutral nitrogen, oxygen, and noble gas emissions. Recent reviews describe this potential.<sup>1,2</sup>

We have completed the adaption of an existing Extreme Ultraviolet (EUV) sounding rocket payload<sup>3-5</sup> for planetary applications in the 800–1200 Å wavelength passband. The payload modifications were technically simple—the most important being a new normal incident Rowland circle spectrograph design optimized for our targets. We flew our modified Extreme Ultraviolet Spectrograph (EUVS) payload twice in the summer of 1994, to observe both the planet Jupiter and surrounding Io torus during the collision of comet Shoemaker-Levy 9 (NASA flight 36.121CL), and the planet Venus (NASA flight 36.117CL). The EUV/FUV observations of the cometary collision with Jupiter by this payload were the only impact observations of this event in this important wavelength region. The Venus flight resulted in a >5x improvement in spectral resolution over all Venus EUV/FUV spectra previously obtained.<sup>6</sup> And, in April 1995 we had the opportunity to again fly EUVS to observe the rare lunar occultation of the bright UV star Spica ( $\alpha$  Virginis, spectral type B0V) to study the presence of various gas constituents that are either known, or may exist in the tenuous lunar atmosphere (NASA flight 36.137CL).<sup>7</sup>

A detailed description of the EUVS instrument and its ground calibration are described in the following two sections (§§ 2 and 3), followed by a summary of the last three EUVS flights in section 4. Conclusions are presented in section 5.

## 2. THE EXTREME ULTRA VIOLET SPECTROGRAPH PAYLOAD

### 2.1 Payload Configuration

The EUVS payload consists of the following main components: a Wolter Type II grazing incidence telescope with an attached NASA supplied vacuum door assembly, a 0.4-m normal incident Rowland circle spectrograph, the science detector (a 2-D imaging photon-counting detector) located at the focal plane of the spectrograph, a NASA supplied fine-guidance camera, the flight electronics, and various support systems. Five skin sections contain the entire payload. The location of each of these components is shown in the mechanical layout of the payload in Figure 1. The forward end of the payload is at the end of the main electronics section; the aft end is at the vacuum door end of the telescope section. The overall length of the payload is 3.175 m (10.42 ft.); the total mass (without the star tracker and shutter door) is 183 kg (404 lbs).

Light at wavelengths less than 1040 Å will not transmit through any known solid substance, so the entire optical train of the EUVS instrument employs only reflective optics.<sup>8</sup> In addition, the opacity of air at these EUV/FUV wavelengths is high; hence, to minimize atmospheric attenuation during ground operation the entire EUVS optical train must be kept under high-vacuum ( $< 10^{-5}$  Torr). This low pressure also insures safe operation of the science detector, which requires high-voltage (-6 kV) for proper operation. During flight, the shutter door at the entrance aperture of the instrument is opened above an altitude of ~100 km exposing the entire EUVS optical train to the high vacuum of space. The high-vacuum of space above 100 km provides a safe environment for operation of the instrument; furthermore, at altitudes >180 km telluric UV absorption and airglow emissions by the earth's atmosphere is minimized at these EUV/FUV wavelengths.

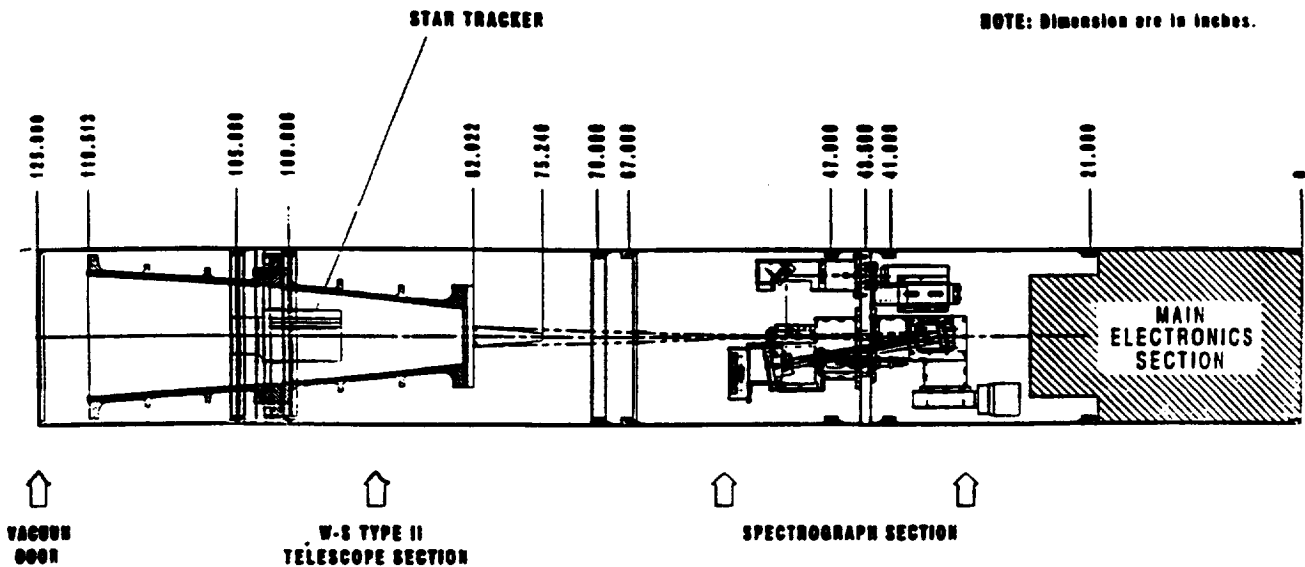
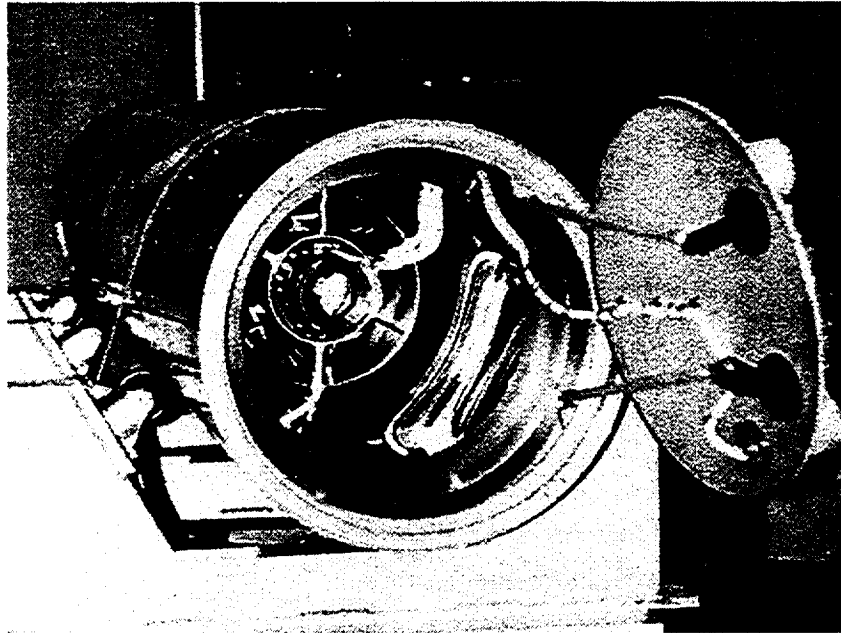


Figure 1. Cross-sectional schematic showing the opto-mechanical layout of the EUVS payload.

Light enters the entrance aperture of the EUVS telescope and is focused onto the entrance slit of the spectrograph. Light that passes through the slit hits the reflective diffraction grating where it is dispersed and reflected back to a best spectral focus at the location of the 2-D imaging science detector. The detector and associated electronics records each detected photon event within the 2-D spectral image, and the telemetry electronics relays the event address of each stimulated pixel to the ground during the flight. Table I summarizes the opto-mechanical characteristics of the EUVS payload.

## 2.2 The Wolter Type II Grazing Incidence Telescope

The Wolter Type II telescope is a diamond-turned  $f/15$  grazing incidence telescope with an entrance aperture 30 cm in diameter.<sup>3,5</sup> A photograph looking into the front end of the telescope is shown in Figure 2. The primary parabolic mirror of the telescope is made of two sections, both of which are bolted to the telescope bulkhead flange located at the center-of-mass of the telescope. The telescope's hyperbolic secondary is attached to the forward end of the primary mirror assembly. Both the primary and secondary mirror assemblies are thermally isolated from the skin sections. A special mounting bracket that holds the star-tracker camera (used to acquire and track the guide stars/planets during the flight) is attached to the telescope bulkhead flange (see Figures 1 and 2).



**Figure 2. Photograph of the front entrance aperture of the EUVS telescope with the NASA supplied shutter door open (right). The NASA supplied Star Tracker is shown mounted inside the telescope. The nickel-coated primary grazing mirror is also shown surrounding the Star Tracker.**

The mirrors are made of 6061-T6 aluminum, overcoated with polished electroless nickel. The secondary has a 250 Å thick coating of sputtered silicon carbide (SiC) over the electroless nickel. The measured effective area of the telescope is 350 cm<sup>2</sup> at 1000 Å; the telescope focuses 50% of the energy from a distant point source into a 40 arc-second diameter spot.<sup>5</sup>

The EUVS telescope has flown successfully on 10 sounding rocket flights: twice in Australia as part of the 1987a supernova campaign, and eight times at White Sands Missile Range (WSMR). The telescope has survived all 10 flights without damage.

## 2.3 The EUVS Rowland Circle Spectrograph

The EUVS spectrograph is a normal incidence 0.4-m Rowland Circle vacuum spectrograph designed and built at Southwest Research Institute in 1993-1994. The mechanical layout of the spectrograph is shown in Figure 3. A spherical reflection grating, with a radius-of-curvature of 400.7 mm, is attached to a ball-bearing/socket center pivot type mounting fixture that allows tip and tilt adjustment of the grating. The 400.7 mm diameter Rowland circle (the dashed circle in Figure 3) passes through the grating center, the entrance slit, and the detector. The surface normal at the center of the grating points to the center of the detector, so that the wavelength at the mid-point of the spectral passband has a diffraction angle near zero. Two different diffraction grating ruling densities have been used with this spectrograph: 1) an 1800 groove mm<sup>-1</sup> grating that gives a plate factor,  $d\lambda/dl$ , of 13.9 Å mm<sup>-1</sup> at the focal plane (used on NASA flights 36.117 to observe Venus, and 36.121 to observe the Jupiter/Io torus system); and 2) a 2400 groove mm<sup>-1</sup> grating that gives a slightly lower plate factor of 10.4 Å mm<sup>-1</sup> for increased dispersion (NASA flight 36.137 to observe Spica during the lunar occultation).

The grating, entrance slit, and detector are housed in two vacuum-tight enclosures made of machined 6061 aluminum. Each enclosure is mounted with an O-ring vacuum seal to the spectrograph bulkhead (see Figure 3). The grating mounting assembly is attached to the forward enclosure, and the aperture slit and detector are mounted in the aft enclosure. A butterfly valve attached to the forward spectrograph housing is the vacuum pump-out port for the entire payload. The payload vacuum enclosure includes everything between the spectrograph bulkhead and the telescope shutter door (see Figure 1). The butterfly valve is closed before flight when the proper vacuum level is reached inside the payload ( $< 5 \times 10^{-6}$  Torr). A  $240 \text{ L s}^{-1}$  external turbo-pump is suitable for pumpdown of the payload to this vacuum level, and is attached to the valve via an access door in the rocket skin.

Two getter pumps attached to the spectrograph bulkhead and protruding into the vacuum section of the payload are used to maintain a high vacuum inside the payload after the turbo-pump has been separated before launch and during the flight (see Figure 3). An ion pump, used to monitor the internal pressure inside the payload during ground checks, is also mounted to the spectrograph bulkhead. A photograph showing the spectrograph housing and entrance slit assembly is shown in Figure 4.

**Table I. Opto-Mechanical Characteristics of the EUVS Sounding Rocket Payload**

<b>Telescope</b>	
Type:	Wolter Type II grazing incidence
Focal Ratio:	f/15
Focal Length:	4619 mm
Entrance Aperture:	30 cm dia.
Effective area at 1000 Å:	350 cm <sup>2</sup>
Plate Scale:	22.4 microns (arc-sec) <sup>-1</sup>
Optical Coatings:	Electroless polished Ni (primary) SiC (secondary)
Length:	55 inches
Weight:	167 lbs
<b>EUVS Spectrograph</b>	
Type:	Normal Incidence Rowland Circle
Grating	
Surface Figure:	Spherical
Radius-of-Curvature:	400.7 mm
Ruled Area:	3 x 3 cm <sup>2</sup>
Angle-of-Incidence:	10.160 degrees (flights 36.117 & 36.121) 12.362 degrees (flight 36.137)
Optical Coating:	SiC (flights 36.117 & 36.121) Ir (flight 36.137)
Blaze Angle:	5 degrees ( $\lambda_{\text{blaze}} = 965 \text{ Å}$ )
Ruling Frequency:	1800 grooves mm <sup>-1</sup> (flights 36.117 & 36.121) 2400 grooves mm <sup>-1</sup> (flight 36.137)
Linear Dispersion:	13.9 Å mm <sup>-1</sup> (flights 36.117 & 36.121) 10.4 Å mm <sup>-1</sup> (flight 36.137)
Wavelength Range:	820 – 1140 Å (flights 36.117 & 36.121) 919 – 1140 Å (flight 36.137)
Field-of-View:	44.6 x 100 (arc-sec) <sup>2</sup> ; 22.3 x 100 (arc-sec) <sup>2</sup> (flight 36.117) 100 x 380 (arc-sec) <sup>2</sup> (flight 36.121) 2.3 x 445 (arc-sec) <sup>2</sup> (flight 36.137)
Detector	
Type:	Open-structure Ranicon (resistive anode)
Format:	25-mm diameter active area
PSF:	65 x 65 mm <sup>2</sup>
Operating Voltage:	6000 V
Photocathode:	KBr
Weight:	97 lbs (includes detector, detector electronics, and FGC <sup>†</sup> )

† - Fine Guidance Camera (see §2.5)

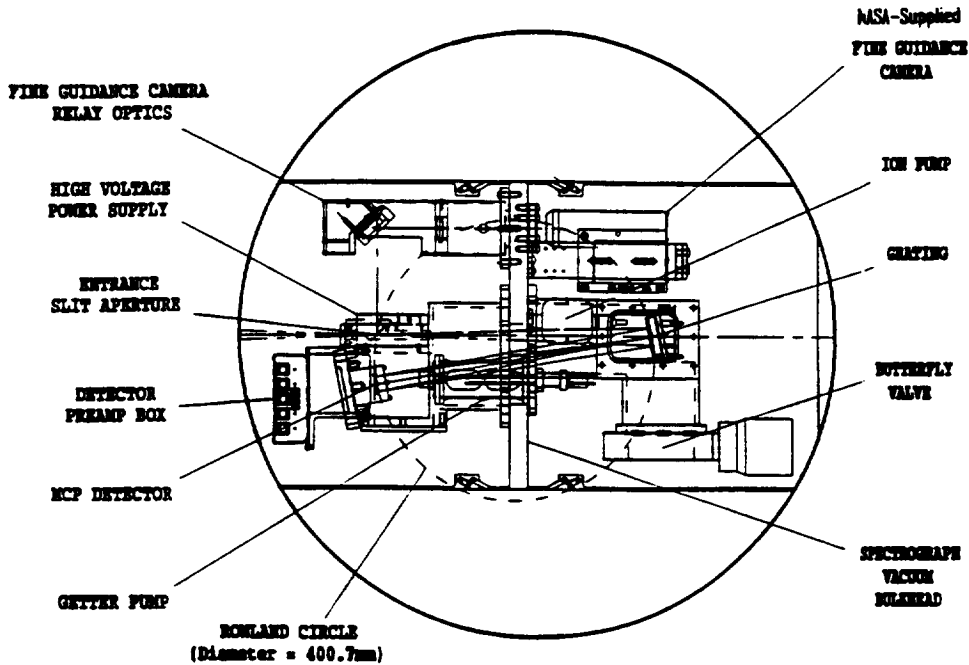


Figure 3. Opto-mechanical layout of the EUVS spectrograph.

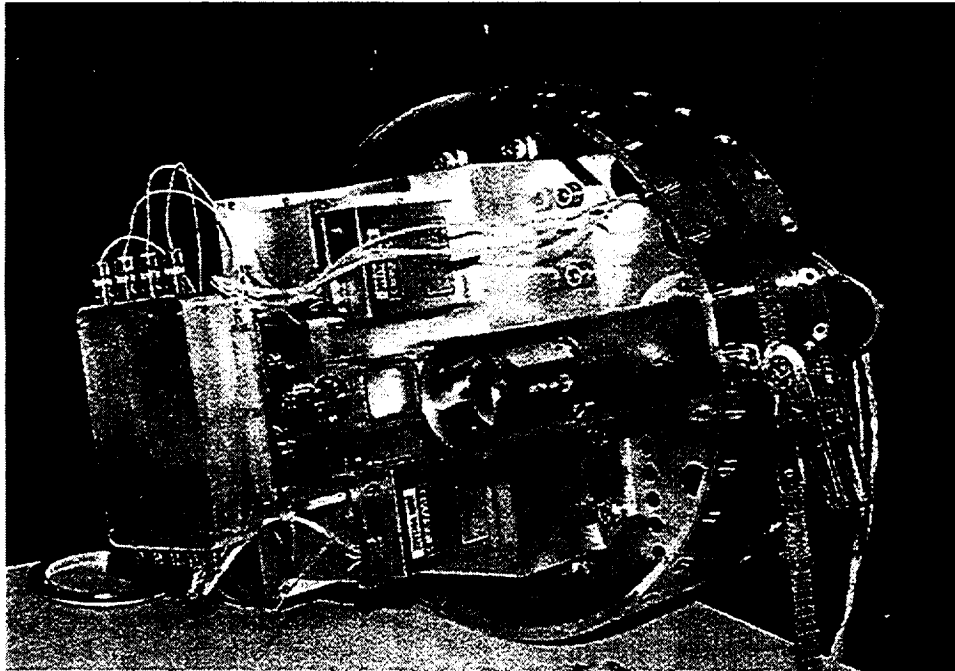


Figure 4. Photograph of the EUVS spectrograph section set up for laboratory functional tests. A LiF viewing port (to allow testing in the laboratory) is shown mounted to the entrance slit assembly located near the center of the photograph. The 4.5-inch ConFlat™ detector flange is shown mounted behind the detector preamp box on the left side of the photograph. The Fine Guidance Camera (FGC) relay optics are located in the cylindrical tube protruding through the bulkhead flange on the right side of the photograph. The two redundant high-voltage power supplies can be seen mounted above and below the entrance slit assembly.

## 2.4 The Science Detector

The science detector at the focal plane of the spectrograph (see Figure 3) is a 2-D resistive anode (Ranicon) photon-counting detector utilizing five microchannel plates (MCPs) arranged in a chevron/Z-stack configuration.<sup>4, 9</sup> The resistive anode readout allows two-dimensional imaging of 1024 x 1024 pixels across the 25-mm diameter active area of the detector. The input surface of the MCP chevron stack is coated with an opaque potassium bromide (KBr) photocathode for enhanced quantum efficiency (QE) within the EUV/FUV passband of the instrument.<sup>10</sup> The detector tube body was designed and built at the Center for Astrophysics and Space Astronomy (CASA) at the University of Colorado in Boulder.<sup>4</sup> We replaced the existing KBr coated MCP in the Ranicon with MCPs freshly coated with KBr before flights 36.121 and 36.117. The DQE of the Ranicon was measured after each deposition.

The rear of the detector body is mounted to a standard 4.5-inch diameter ConFlat™ flange, which in turn is mounted to the aft spectrograph enclosure (see Figures 3 and 4). Two EMCO high-voltage power supplies that are diode-or'd together provide redundant high-voltage to operate the detector MCP stack. The detector preamplifiers are housed in their own separate box attached to the back of the spectrograph aft enclosure, behind the detector (see Figure 4). Hermetic feedthroughs are used to pass low voltage power and signals from the preamplifier electronics through the spectrograph bulkhead to the main electronics section.

## 2.5 The Fine Guidance Camera (FGC)

A NASA-supplied intensified CCD visible light video camera is used to image the spectrograph entrance slit, and allows for fine pointing guidance during flight. This Fine Guidance Camera (FGC), a Xyberon Model ISS-255, is mounted to the forward side of the spectrograph bulkhead. A flat mirror and lens relays and focuses the light from the slit plane onto the FGC focal plane through a 2.75-inch ConFlat viewing port that is mounted to the spectrograph bulkhead (see Figures 3 and 4). This optical relay, designed and built by Southwest Research Institute, provides a 10-arc min diameter field-of-view (FOV) of the slit plane during ground and flight operations.

The video signal from the camera is relayed down to the ground during flight for real time display of the slit and targets that enter the FOV of the EUVS telescope. This makes it possible for real-time ACS uplink commands to be sent during the flight by the experimenter to keep the target centered on the slit. Two LED light sources mounted to the aft spectrograph enclosure are used to illuminate the slit plane for visual inspection during ground testing and flight. They can be turned on and off during flight by uplink command.

## 2.6 Payload Electronics

The EUVS electronics are located in three sections of the payload: the main electronics section, the spectrograph section, and the telescope section. A separate GSE console allows operation of the payload during ground and pre-launch testing.

The main electronics section is located in the non-vacuum section of the experiment at the forward end of the payload (see Figure 1). This section contains the system battery, the telemetry interface box, a power distribution box, the Ranicon detector's pixel position computer, high-current drive relays, barometric switches, and a skin temperature monitor. The Ranicon pixel position computer converts the detector analog output signal from the preamplifiers into (x, y)-pixel address pairs; each word is 10-bits in length. Each (x, y)-event pair (one pair per detected photon event) is fed into the telemetry digital data stream via the telemetry (TM) interface box.

The TM interface box is capable of outputting the digital science data at the standard data rates of 400 and 800 kbps, and has been recently modified and flown for output at 10 Mbps. It also is capable of outputting to the NASA encoder up to 41 analog housekeeping signals for monitoring the health and status of various EUVS instrument functions during ground and flight operations.

The spectrograph section contains the Ranicon detector, the detector preamplifiers, two redundant high-voltage power supplies, a high-voltage diode mixing box, and two LEDs to illuminate the entrance slit for the FGC.

The telescope section contains the vacuum shutter door control and motor, and the star tracker. The star tracker is sometimes used to acquire and track mission targets (that meet specific brightness and location criteria) during a sounding rocket flight.



### 3. CALIBRATION

The EUVS instrument was calibrated for effective area and wavelength scale at the University of Colorado's CASA facilities prior to the two flights conducted in the summer of 1994. The entire EUVS payload was inserted into the CASA "Long-Tank" vacuum chamber and illuminated with collimated EUV/FUV light from a hollow-cathode discharge source.<sup>11, 12</sup> The 60-cm diameter newtonian collimator inside the "Long-Tank" easily overfilled the EUVS' 30-cm diameter entrance aperture. The photograph in Figure 5 shows the EUVS payload being readied for insertion into the "Long-Tank" for calibration.

The effective area of the EUVS instrument was measured at various wavelengths across the EUVS' spectral passband using the emission lines of argon at 919 and 1048 Å, and oxygen at 834 and 989 Å. The 1800 groove mm<sup>-1</sup> grating was installed in the EUVS' spectrograph at the time of calibration. A Wadsworth spectrograph, calibrated against an NBS calibrated photodiode, was used to measure the flux entering the EUVS telescope from the collimator. The measured effective area of the EUVS instrument for flight 36.121 (target-Jupiter/Io torus system) varies from a minimum of 0.2 cm<sup>2</sup> at 834 Å to 1.7 cm<sup>2</sup> at 1048 Å.

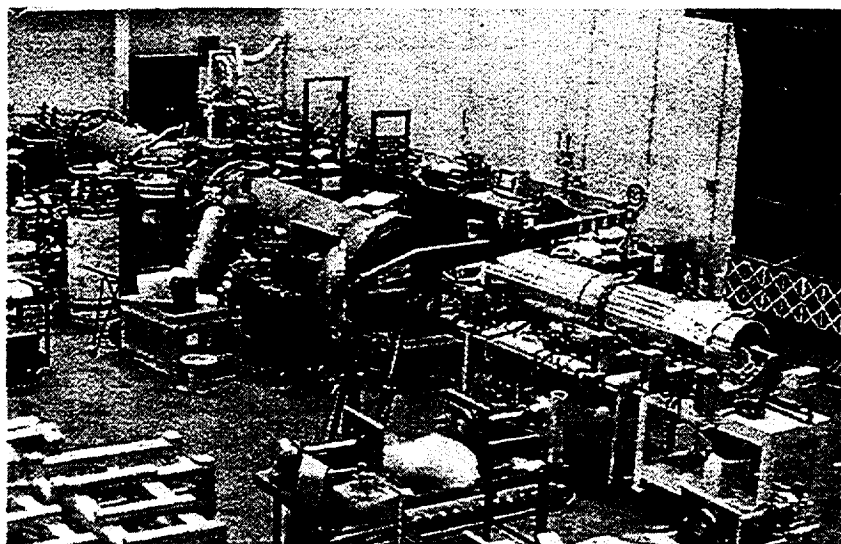


Figure 5. Photograph of the "Long-Tank" calibration facility at the University of Colorado in Boulder. The "Long-Tank" vacuum chamber is located in the upper left of the photograph. The EUVS payload (right side of photograph) is being readied for insertion into the "Long-Tank" for photometric calibration.

### 4. EUVS LUNAR AND PLANETARY MISSIONS

The EUVS sounding rocket payload, in its present configuration, has successfully flown on three NASA sounding rocket flights from White Sands Missile Range (WSMR), New Mexico. Before each flight, the EUVS payload was integrated and tested with the flight support hardware (i.e., telemetry system, attitude control system, S-19 boost guidance system, recovery system, nosecone, etc.) at WSMR before final integration with the launch vehicle (Black Brant IX, see below) at the launch rail. Table II summarizes the EUVS instrument and flight parameters for each of these three NASA sounding rocket flights. A detailed discussion of each of these flights follows in the remaining part of this section.

#### 4.1 Comet SL 9 Impact with Jupiter

At 05:53 UT on July 20, 1994 the EUVS payload was successfully launched on a Black Brant IX sounding rocket from WSMR. The objective of this flight (NASA 36.121CL) was to obtain EUV/FUV spectra (820-1140 Å) of Jupiter and the Io plasma torus during the comet Shoemaker-Levy 9 (SL-9) impacts in order to assess the effects of the penetration of the SL-9 nuclei through the Jovian magnetosphere and their affect on the Jupiter system.<sup>13</sup>

The EUVS spectrograph entrance slit for this flight was 380 arc-sec in length in the spatial dimension, and 100 arc-sec in width in the spectral dimension. The slit length corresponded to 20.7 Jupiter radii ( $R_J$ ); the slit width corresponded to a spectral resolution of 27.7 Å (FWHM). Since we did not know, a priori, whether or not the SL-9 impacts would increase or

decrease the emissions from Jupiter and the Io torus, we chose to configure the EUVS with a rather large slit width to maximize the total flux entering the spectrograph. This decision sacrificed spectral resolution, but insured that the entire Io torus was imaged onto the detector. During the flight, Jupiter was centered in the slit, and the slit was oriented so that the long axis of the slit was parallel to Jupiter's equator.

<b>Table II. EUVS Sounding Rocket Flight Summary Table</b>			
<b>EUVS Flight Parameter</b>	<b>NASA Flight # 36.121CL</b>	<b>NASA Flight # 36.117CL</b>	<b>NASA Flight # 36.137CL</b>
Date:	20 July 1994	16 August 1994	15 April 1995
Launch Time:	05:53:01 UT	03:25:01 UT	10:07:42 UT
Launch Vehicle:	Black Brant IX	Black Brant IX	Black Brant IX
Mission Target:	Jupiter/Io torus system	Venus	Spica near lunar limb
Science Objectives:	Study EUV/FUV emissions from Jupiter/Io torus system during comet SL-9 impact w/ Jupiter.	Study EUV/FUV emissions from planet Venus.	Study presence of various gas constituents in the lunar atmosphere.
Photometric Calibration Target:	Spica	Spica	Spica
EUVS Configuration:	1) 1800 gr mm <sup>-1</sup> grating 2) SiC coating on grating 3) Fresh KBr photocathode	1) 1800 gr mm <sup>-1</sup> grating 2) SiC coating on grating 3) Fresh KBr photocathode	1) 2400 gr mm <sup>-1</sup> grating 2) Ir coating on grating 3) Long, narrow slit
EUVS Wavelength Range:	820 - 1140 Å	820 - 1140 Å	919 - 1140 Å
Entrance Slit FOV:	100 x 380 (arc-sec) <sup>2</sup>	22.3 x 100 (arc-sec) <sup>2</sup> 44.6 x 100 (arc-sec) <sup>2</sup>	2.3 x 445 (arc-sec) <sup>2</sup>
EUVS Effective Area at 1050 Å <sup>†</sup> :	1.7 cm <sup>2</sup>	2.0 cm <sup>2</sup>	0.6 cm <sup>2</sup> <sup>†††</sup>
Altitude at Apogee:	264 km	255 km	259 km
Time on Mission Target (>200 km):	224 s	210 s	235 s
MET at Apogee:	T+265 s	T+261 s	T+262 s
Total Accumulated Science Counts on Mission Target:	5860	1532	> 3 x 10 <sup>6</sup> <sup>††</sup>
Gyro Update Targets	Not Required	Vega Arcturus	Jupiter Arcturus
ACS Guidance Mode	Jupiter: Star Tracker Spica: Star Tracker	Vega: Star Tracker Arcturus: Star Tracker Venus: Gyros Only Spica: Gyros Only	Jupiter: Star Tracker Arcturus: Star Tracker Spica: Gyros Only
Mission Success	Successful	Successful	Successful

† Effective area includes slit transmission.

†† 800 kbps TM

††† Effective area is lower due to thinner slit width.

The EUVS flight occurred at a time between the SL-9 fragment L impact (which occurred 8 hours earlier) and the fragment N impact (which occurred 4 hours after the flight). Jupiter was observed during the flight between a mission elapsed time (MET) of T+115 s (162 km altitude, upleg portion of flight trajectory) and T+390 s (193 km altitude, downleg portion of flight trajectory). EUVS reached a flight apogee of 264 km. At apogee, the apparent Jupiter system III central meridian longitude was 166 degrees. Following the observation of Jupiter, the EUVS instrument observed the bright UV star Spica, for in-flight calibration purposes, from T+395 s (189 km altitude, downleg) to T+450 s (108 km, downleg). The spectrum obtained from observing Spica allowed us to establish an absolute effective area calibration of the EUVS payload between 912 Å (the

short wavelength cutoff of Spica's spectrum due to interstellar absorption) and EUVS' long wavelength cutoff at 1140 Å. The absolute effective area of EUVS was hinged on the FUV spectral data of Spica taken by the Voyager 2 UVS instrument.<sup>14</sup>

Figure 6 shows the 2-D Jupiter/Io torus count spectrum obtained by EUVS between T+146 and T+370 seconds. In this period of time the EUVS payload was above 200 km where the amount of detectable telluric absorption was minimal. A total of 5860 counts were obtained from the Jupiter system during this interval. The counting statistics and imaging performance of the data were sufficient to resolve the disk of Jupiter and both the east (dawn) and west (dusk) ansa of the torus. The three brightest spectral features in the spectrum in the Io torus regions are identified emissions from O II/O III at 834 Å, and S II at 910 Å and 1046 Å. Other features evident in Figure 6 have not yet all been identified; however, H I emission at 1026 Å (Ly β), and the "continuum" feature at wavelengths > 912 Å, which has been identified as the H<sub>2</sub> Lyman band, come from the disk of Jupiter itself.

Post-flight analysis of the data has been performed including the conversion of the raw count spectrum to a brightness spectrum. A thorough discussion of this data, including the data reduction and calibration techniques applied to the data can be found in Stern *et al.* 1995.<sup>13</sup>

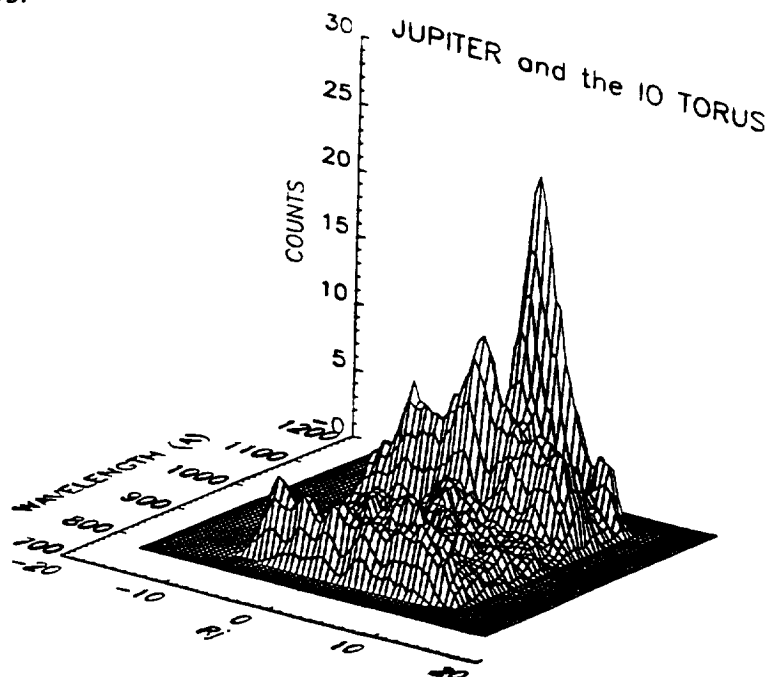


**Figure 6. The integrated Jupiter/Io torus system count spectrum obtained by EUVS, after instrument background counts have been removed. The two ansa of the Io torus and Jupiter itself are each clearly distinguishable.**

#### 4.2 Venus

At 03:25 UT on August 16, 1994 the EUVS payload was again successfully launched on a Black Brant IX sounding rocket from WSMR. The objective of this flight (NASA 36.117CL) was to obtain EUV/FUV spectra (820-1140 Å) of Venus' upper atmosphere at a spectral resolution 5x higher than that yet obtained at the time of this flight ( $\Delta\lambda \sim 7$  Å FWHM).<sup>6</sup>

The EUVS spectrograph entrance slit for this flight was 200 arc-sec in overall length in the spatial dimension, with two 100 arc-sec sections of differing widths. One width was 44.6 arc-sec, corresponding to a spectral resolution of 14 Å FWHM; the other width was 22.3 arc-sec, corresponding to a spectral resolution of 7 Å FWHM. The wider portion of the slit allowed us to record spectral data at twice the throughput with a sacrifice of half the spectral resolution. During the flight, the disk of Venus was first placed over the wide portion of the slit for 96 s, then over the narrow portion of the slit for 145 s.

Because of the proximity of the Sun to the horizon (~ 4 degrees) as seen from the rocket at apogee (255 km) during the flight, and the close proximity of the Sun from Venus (~45 degrees), the Star Tracker could not be used to acquire Venus. Instead, the attitude control system gyros were used to guide the payload to Venus after two gyro update maneuvers were made to Vega and Arcturus using the Star Tracker.

Venus was observed during the flight between an MET of T+163 s (212 km altitude, upleg portion of flight trajectory) and T+404 s (162 km altitude, downleg portion of flight trajectory). EUVS reached a flight apogee of 255 km. Following the observation of Venus, the EUVS instrument observed the star Spica for in-flight calibration purposes, from T+416 s (145 km altitude, downleg) to T+446 s (99 km, downleg).

Figure 7 shows the accumulated raw spectrum of Venus in the wide slit between T+163 s and T+370 s MET after removal of background events. In this period of time the EUVS payload was above 200 km where the amount of detectable telluric absorption was minimal; however, modelling of the expected telluric background shows contribution at three wavelengths in this spectrum: 834 Å (O II), 911 Å (H I), and 1026 Å (H I/O I). A total of 1532 counts were obtained in both the wide and narrow slits from Venus during this interval. At this time we are still analyzing the flight data and are in the process of identifying the spectral features evident in the spectrum. We plan to publish our results later this year.

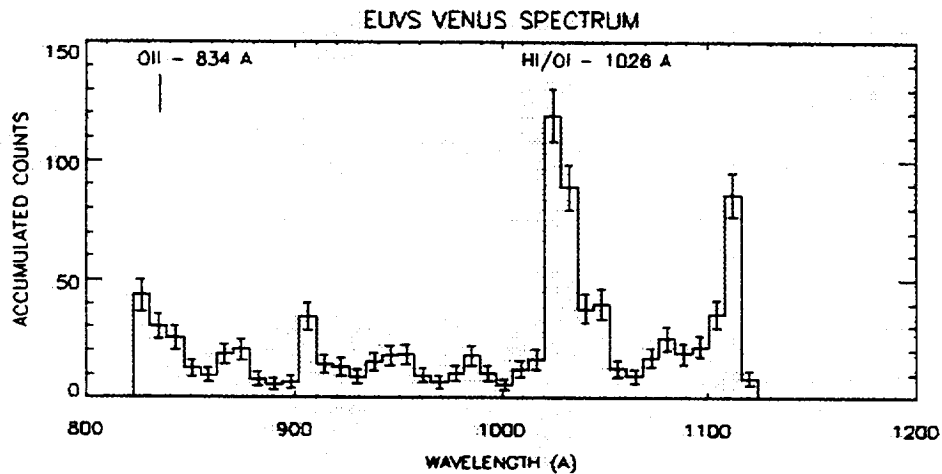


**Figure 7. The accumulated raw count EUV/FUV spectrum of Venus atmosphere from the wide slit (44.6 arc-sec FOV) after removal of background events. The amplitude of the telluric emission features have not been subtracted from this data (the most significant to this data set is due to H I/O I at 1026 Å). Each spectral bin is 7.9 Å wide. The error bars represent the  $\pm 1\sigma$  count levels.**

### 4.3 Spica/Lunar Atmosphere Occultation

On April 15, 1995 we had the opportunity to observe a rare lunar occultation of the bright UV star Spica with the EUVS payload in an attempt to investigate the composition of the lunar atmosphere. Spica, being one of the ten brightest 900-1100 Å sources in the sky, and the brightest such source in the ecliptic, provided the best possible background source of known FUV emission to look for characteristic absorption features due to possible atmospheric constituents in the lunar atmosphere including atomic oxygen O I (989 Å) and H I (Ly  $\beta$  1025 Å, Ly  $\gamma$  972 Å), molecular N<sub>2</sub> (via the c<sub>4</sub>' bands near 960 Å), O<sub>2</sub> (via the H-X system), and CO (via the F-X system). Of prime importance, the occultation also allowed us to search for absorption features in Spica's FUV spectrum due to neutral Ar I at 1048 and 1066 Å. Ar I was detected by the Apollo 17 LACE surface mass spectrometer, but on every occasion, the LACE Ar channels saturated just after sunrise (when the Ar number density exceeded  $4 \times 10^4 \text{ cm}^{-3}$ ), thus preventing an accurate estimate of the Ar number density.<sup>7</sup>

In order to improve the chances of detecting the extremely narrow absorption features ( $\Delta\lambda \sim 4\text{-}5 \text{ mÅ FWHM}$ ) that any of the above gases would create in the Spica continuum spectrum, the EUVS spectrograph was refitted with a grating of higher groove density ( $2400 \text{ gr mm}^{-1}$ ) to increase the spectral dispersion. With this improved dispersion (corresponding to a plate scale at the focal plane of  $10.4 \text{ Å mm}^{-1}$ ), in combination with a spectrograph slit-width of  $50 \text{ μm}$  (2.2 arc-sec), the EUVS spectrograph now performed with a spectral resolution  $\lambda/\Delta\lambda \sim 1200$  at 1048 Å.

In addition to the higher dispersion required for this flight, we also needed to record as many photon events from Spica as possible to provide a high enough signal-to-noise ratio to allow us to detect the presence of any of these extremely narrow absorption features if they exist. To estimate the detector output count rate with the new grating and slit assembly, we needed to recalibrate the instrument. We did not have time before the flight to calibrate EUVS in the CASA "Long-Tank" facility; we

instead calibrated the grating and the transmission of the slit separately, and used the results of each to calculate the new effective area of the instrument ( $0.6 \text{ cm}^2$  at  $1048 \text{ \AA}$  including slit transmission). The effective area values were then used, along with the measured FUV flux values of Spica obtained by Voyager 2, to compute the expected count rate from Spica during the flight.<sup>14</sup> With a TM downlink rate of 800 kbps, the expected output count rate was  $21.5 \text{ kevents s}^{-1}$ ; with the faster TM rate of 10 Mbps, the expected output count rate was  $58.4 \text{ kevents s}^{-1}$ . In 200 seconds of data taking time, an estimated  $4.3 \times 10^6$  counts at 800 kbps (and  $11.7 \times 10^6$  counts at 10 Mbps) would be recorded during the flight.

The primary and backup launch windows were carefully chosen so that the EUVS payload would observe Spica pass through the lunar atmosphere up to the lunar limb, where the atmosphere would have the highest column density. The primary window was targeted to observe Spica disappear behind the Moon (ingress portion of occultation) at an altitude of  $\sim 160 \text{ km}$  on the downleg portion of the rocket's trajectory; the backup window, which occurred about 1 hour later, was targeted to observe Spica reappear from behind the Moon (egress portion of occultation) at an altitude above  $200 \text{ km}$  on the upward portion of the rocket's trajectory. Because of the close distance of the Moon to the Earth, the parallax between the Earth and Moon had to be taken into account along the rocket's trajectory in order to properly predict the time of disappearance and reappearance as seen by the EUVS payload during flight. Professor Mitsuru Soma, from the National Astronomical Observatory of Japan, performed the position calculations of the Moon's limb with respect to Spica for the predicted rocket trajectory. Based upon these calculations, we were able to select the launch times for both the primary and backup windows.

The primary launch window was open for a period of only 90 seconds, with an optimum launch time of 10:07:41 UTC. Launching at this time would give us  $\sim 235 \text{ s}$  of Spica data before Spica disappeared behind the Moon (which would occur at an altitude of  $\sim 148 \text{ km}$ ). The backup launch window was open for a period of only 60 seconds, with an optimum launch time of 11:09:41 UTC. This window would give us  $\sim 289 \text{ s}$  of Spica data from reappearance to shutter door closure.

EUVS was launched successfully on a Black Brandt IX sounding rocket from WSMR at 10:07:42 UT on April 15, 1995 (within 1 second of the optimum launch time in the primary launch window). After despin and sustainer separation, the attitude control system in conjunction with the NASA star tracker (located inside the EUVS telescope, see Figure 2) maneuvered the payload to point at Jupiter, followed by a maneuver to point at Arcturus. These two "guide star" maneuvers were required to update the gyros inside the ACS so that the final maneuver to our primary target, Spica, could be made using only the gyros (the star tracker could not be used because of the proximity of the Moon to Spica; the Moon's high brightness would saturate the star tracker making it useless). The payload settled on Spica at an MET of T+160 and 235 s before the time of disappearance. After Spica was acquired, uplink corrections were repeatedly sent to the payload from the ground to keep Spica centered on the slit. The peak output count rate during the flight was very close to that predicted:  $\sim 18\text{-}20 \text{ kevents s}^{-1}$  (with the 800 kbps TM data stream). The payload reached an apogee of  $259 \text{ km}$  at T+262 s.

The extreme brightness of the Moon in the visible compared with Spica, and the proximity of Spica with the Moon's limb caused the automatic gain control of the FGC to lower its intensifier voltage, and thus its gain, to protect the intensifier tube from damage due to the high input light flux. At the lower gain, the FGC was no longer able to detect the light from Spica; hence, pointing the instrument required using the science detector count rate as a guide (since the brightness of Spica in the FUV is  $> 1000$  times that of the Moon). This was anticipated before the flight, and this strategy worked out well for keeping Spica centered on the slit.

Spica disappeared behind the Moon at T+394 s, within just a few seconds of the time predicted (T+392 s). Uncertainties in the actual flight trajectory account for this discrepancy. The science count rate dropped instantaneously at disappearance from  $18\text{-}20 \text{ kevents s}^{-1}$  to the background rate of  $\sim 5\text{-}10 \text{ events s}^{-1}$ . At this time the payload was maneuvered to point at the center of the Moon to collect FUV data of the Moon until T+450 s when the shutter door was closed and payload power was shut off. After power shutdown, the payload was spun up for re-entry, followed by parachute deployment and touchdown. The payload was successfully recovered the morning of 15 April 1995 at first light. Approximately 24 hours after recovery, the payload was found to still be under partial vacuum at  $\sim 1 \text{ mTorr}$ , meaning that no significant leaks developed during the flight or at touchdown. The payload was pumped to  $2 \times 10^{-6} \text{ Torr}$  with the payload vacuum pumpcart and turned on, and a Pt spectrum taken to check for any motion of the grating. The Pt spectrum matched that taken before flight (to  $\pm 1 \text{ pixel} = \pm 0.2 \text{ \AA}$ ), hence no motion occurred during flight.

Data from both the 800 kbps and the 10 Mbps TM links were successfully recorded and the data is now undergoing analysis for lunar atmospheric absorption features, interstellar absorption features, and features in the spectrum due to Spica itself. In addition, the spectral data we obtained of the Moon after the disappearance of Spica is being used to extract a lunar albedo in the EUV/FUV. We plan to publish these findings soon.

## 5. CONCLUSIONS

We have completed modifications of an existing EUV/FUV telescope/spectrograph sounding rocket payload for planetary observations in the 800 - 1200 Å wavelength band, and have successfully flown this modified instrument 3 times within the past year to observe the Jupiter/Io torus system during the comet Shoemaker-Levy 9 collision in July 1994, the planet Venus in August 1994, and the lunar occultation of Spica on April 15, 1995. The modifications included designing and building a new 0.4-m Rowland Circle spectrograph for the payload.

With the modified EUVS instrument, we now have a unique, pre-FUSE capability that can be exploited for the remote sensing of planetary and cometary atmospheres. No existing space observatory operates in this important 800-1200 Å spectral bandpass—this makes EUVS a unique resource. We hope to continue to fly this invaluable instrument in the future for further planetary and interstellar absorption studies.

## 6. ACKNOWLEDGEMENTS

We wish to thank our field support staff at SwRI including Tom Booker, John McDonald, and Clarence McGuiness. At CU we wish to thank Scott McDonald and Gary Kushner for all of their support during the calibration and integration activities. We also want to thank Dr. Mitsura Soma and Dr. David Dunham for their invaluable assistance in the occultation predictions for the 36.137CL flight. Finally we wish to thank our NASA/Wallops mission managers Bob Spagnuolo (36.121CL) and Frank Lau (36.117CL & 36.137CL), and the entire NASA/contractor team that made the EUVS sounding rocket flights a success. This work was supported under NAG5-5006.

## 7. REFERENCES

1. Bowyer, S. and R.F. Malina, "The Extreme Ultraviolet Explorer Mission," *Adv. Space Res.*, **11** (11), pp. 205-215, 1991.
2. Feldman and Bagenal, "HUT Observations of Comet Levy," *Ap. J. Lett.*, **379**, L37, 1991.
3. Cash, W.C., T.A. Cook, C. Chambellan, D. Heyse, D. Hofmockel, T.P. Snow, and D. Windt, *Exp. Astron.*, **1**, p. 123, 1989.
4. Wilkinson, E., James C. Green, and Webster Cash, "The Extreme Ultraviolet Spectrograph: A Radial Groove Grating, Sounding Rocket-Borne, Astronomical Instrument," *Ap. J.*, **89**, 211, 1993.
5. Wilkinson, E., *Extreme Ultraviolet Opacity Sources in the DA White Dwarf G191-B2B*, Doctoral Dissertation, University of Colorado, 1993.
6. Hord, C.W., C.A. Barth, L.W. Esposito, W.E. McClintock, W.R. Pryor, K.E. Simmons, A.I.F. Stewart, G.E. Thomas, J.M. Ajello, A.L. Lane, R.W. West, B.R. Sandel, A.L. Broadfoot, D.M. Hunten, D.E. Shemansky, "Galileo Ultraviolet Spectrometer Experiment: Initial Venus and Interplanetary Cruise Results," *Science*, **253**, pp.1548-1550, 1991.
7. Morgan, T.H. and S.A. Stern, "Revived Interest in the Lunar Atmosphere," *Eos*, **72**, (20), pp. 225-228, 1991.
8. Samson, James A.R., *Techniques of Vacuum Ultraviolet Spectroscopy*, Pied Publications, Lincoln, Nebraska, 1967.
9. Firmani, C., E. Ruiz, C.W. Carlson, M. Lampton, and F. Paresce, "High resolution imaging with two dimensional resistive anode photon counters," *Rev. Sci. Instr.*, **53**, p. 570, 1982.
10. Siegmund, O.W.H., E. Everman, J. Vallerger, and M. Lampton, "Extreme Ultraviolet Quantum Efficiency of Opaque Alkali Halide Photocathodes on Microchannel Plates," *Optoelectronics Technologies for Remote Sensing from Space*, SPIE **868**, pp. 18-24, 1987.
11. Cook, T. A., W. Cash, and J. C. Green, "Far Ultraviolet Spectrophotometry of BD +28 4211," *Adv. Space Res.*, **11** (11), pp. 29-32, 1991.
12. Paresce, F., S. Kumar, and C. S. Bowyer, "Continuous Discharge Line Source for the Extreme Ultraviolet," *Ap. Opt.*, **10**, p. 1904, 1971.
13. Stern, S.A., D.C. Slater, W. Cash, E. Wilkinson, J.C. Green, and G.R. Gladstone, "Rocket FUV Observations of the Io Plasma Torus During the Shoemaker-Levy/9 Impacts," to appear in *Geophysical Research Letters*, 1995.
14. Holberg, J.B., W.T. Forrester, and D.E. Shemansky, "Voyager Absolute Far-Ultraviolet Spectrophotometry of Hot Stars," *Ap. J.*, **257**, pp. 656-671, 1982.